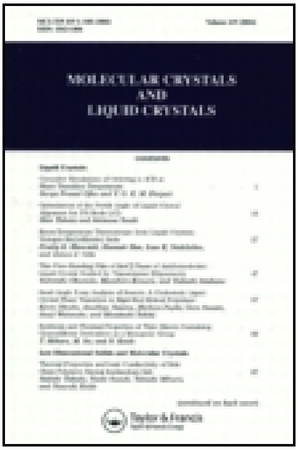

Molecular Crystals and Liquid Crystals
Publication details, including instructions for authors and subscription information:
http://www.tandfonline.com/loi/gmcl20

Optical Methods for Determining Anisotropy of Diamagnetic Susceptibility and Other Material Parameters of Nematics by Using Cells of Varying Thickness

Jerzy Kędzierski [a], Zbigniew Raszewski [a], Jolanta Rutkowska [a], Paweł Perkowski [a], Wiktor Piecek [a], Jerzy Zieliński [a], Marek Andrzej Kojdecki [b], Ludwika Lipińska [c] & Emilia Miszczyk [d]

[a] Institute of Applied Physics, Military University of Technology, Warsaw, Poland

[b] Institute of Mathematics and Cryptology, Military University of Technology, Warsaw, Poland

[c] Institute of Electronic Materials Technology, Warsaw, Poland

[d] Institute of Physics, Radom University of Technology, Radom, Poland

Version of record first published: 31 Aug 2006

Mol. Cryst. Liq. Cryst., Vol. 437, pp. 223/[1467]–241/[1485], 2005

ISSN: 1542-1406 print/1563-5287 online
DOI: 10.1080/15421400590955370

Optical Methods for Determining Anisotropy of Diamagnetic Susceptibility and Other Material Parameters of Nematics by Using Cells of Varying Thickness

Jerzy Kędzierski
Zbigniew Raszewski
Jolanta Rutkowska
Paweł Perkowski
Wiktor Piecek
Jerzy Zieliński
Institute of Applied Physics, Military University of Technology, Warsaw, Poland

Marek Andrzej Kojdecki
Institute of Mathematics and Cryptology, Military University of Technology, Warsaw, Poland

Ludwika Lipińska
Institute of Electronic Materials Technology, Warsaw, Poland

Emilia Miszczyk
Institute of Physics, Radom University of Technology, Radom, Poland

Wedge cells (of the wedge angle of the order of few milliradians) were used for studying Fréedericksz' transition of splay-bend type. The phase shift between ordinary and extraordinary rays of light normally incident on the cell boundary was used as a physical quantity monitoring the state of the director field inside the cell in selected zones equivalent to flat-parallel cells of different thickness. The optical response was measured as a function of a voltage or a magnetic field (or both of them, crossed or parallel). Experiments were performed with two cells, filled with the 4′-pentyl-4-cyanobipfenyl liquid crystal (5CB), of different cover coatings providing strong or weak nematics-substrate coupling. Four different methods were applied for determining the anisotropy of diamagnetic susceptibility of the nematics after results of measurements, separately or simultaneously with the

This work was supported by the Polish Ministry of Scientific Research and Information Technology in years 2004–2005, grant 3T08A03426.

Address correspondence to Jerzy Kędzierski, Institute of Applied Physics, Military University of Technology, 00-908 Warsaw, Poland. E-mail: jkedzierski@hat.edu.pl

splay or bend elastic constants or the nematics-substrate coupling characteristics. The resulting values of material parameters are compared and the features of the methods are commented.

Keywords: 4′-pentyl-4-cyanobipfenyl (5CB); anchoring energy; anisotropy of diamagnetic susceptibility; inverse problem; nematics parameter identification; wedge cell

WEDGE CELL FOR MEASURING OPTICAL CHARACTERISTICS OF NEMATICS

Each wedge nematic cell was made of glass plates (of size 22×35 mm), coated with indium-tin oxide electrodes and orienting layer of polyimide (PM9 or MP2). The plates were glued without a spacer along one edge and with a spacer (of thickness about 200 μm) along the other. The orientation of the nematics molecules (5CB) enforced by substrates was parallel to the boundaries and to the wedge edge. Each cell was placed in a thermostatic stage between the polariser and analyser crossed in the measurement system, consisting of a He–Ne laser and a microscope with a photodetector, and between pole pieces of an electromagnet. In the normally incident light a system of interference fringes appeared, as in schematic Figure 1. In the small neighbourhood of each fringe position a wedge cell can be

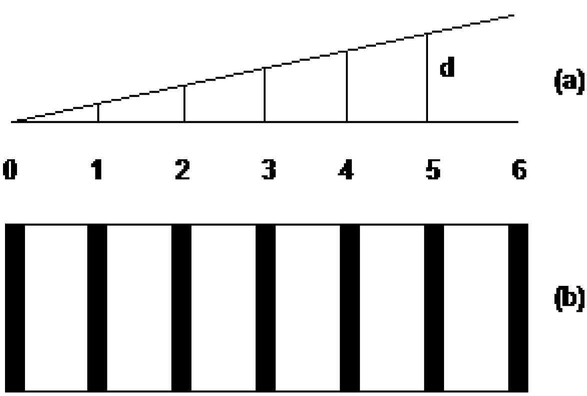

FIGURE 1 System of interference fringes of normally incident light in a wedge cell, filled with a nematics of planar alignment, in the absence of external fields; $\Phi_j = 2\pi\Delta_j\lambda^{-1}$, $d_j = \Delta_j n_a^{-1} = j\lambda n_a^{-1}$, $n_a \equiv n_e - n_0$, where j is the order of an interference minimum (displayed in the figure), d is the corresponding cell thickness, δ is the difference of optical paths, Φ is the phase shift and λ is the light wavelength; a) denotes the side-view-scheme and b) denotes the top view.

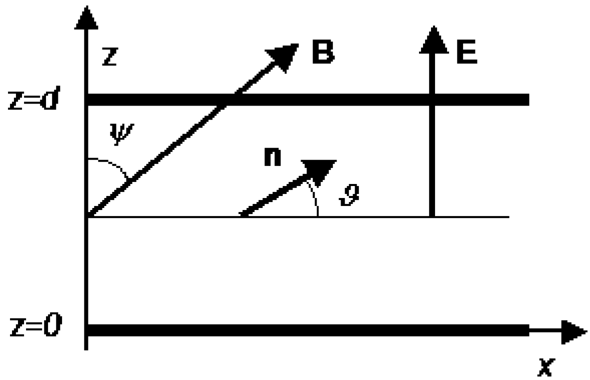

FIGURE 2 Sketch of experimental configuration of a flat-parallel nematic cell in external fields (in Cartesian co-ordinates). The director, *Oz* axis and external (magnetic or electric) field vectors are all in the same plane *Oxz*. The one-dimensional approximation is considered i.e., the physical fields are assumed as depending only on z e.g.: $\vec{n}(z) = (\cos\vartheta(z), 0, \sin\vartheta(z))$, $\vec{E}(z) = (0, 0, E(z))$, $\vec{B}(z) = (B\sin\psi, 0, B\cos\psi)$.

treated as the planar one (like sketched in Fig. 2) due to very small wedge angle. The intensity of normally incident light transmitted through the cell in the positions of selected interference fringes was recorded as a function of applied voltage and magnetic field. In such experiment a wedge cell is equivalent to a system of planar cells of different thickness.

DESCRIPTION OF PHENOMENA

A flat-parallel nematics cell is very well approximated as a flat layer, infinitely extended in two directions (*Ox* and *Oy*), with plane boundaries perpendicular to *Oz* axis in three-dimensional Cartesian co-ordinate system, like sketched in Figure 2. The stationary states of such layer have the form of planar deformations if external field vectors and anchoring direction are all in the same plane (as in Fig. 2). Such stationary states, corresponding to constant voltage and magnetic field can be well described in one-dimensional approximation by the director vector field $\vec{n}(z) = (\cos\vartheta(z), 0, \sin\vartheta(z))$, fully characterised by the tilt angle $\vartheta(z)$ between the director and the layer surface. For a layer of thickness d the total free energy per unit surface area, corresponding to planar strain state, may be represented by the functional:

$$F = \int_0^d f(\vartheta, \vartheta')dz + f_1(\vartheta_1) + f_2(\vartheta_2) \tag{1}$$

where: $f(\vartheta,\vartheta')$ – is the density of the bulk free energy of the nematics elastic deformation and of the interactions of the director field with external electric and magnetic fields, $f = f_K + f_E + f_M$; $f_1(\vartheta_1) + f_2(\vartheta_2)$ – is the surface free energy density in the case of weak (finite) anchoring of nematic molecules on the layer boundaries; $\vartheta' = d\vartheta/dz$, $\vartheta_1 = \vartheta(0)$, $\vartheta_2 = \vartheta(d)$. In the case of strong anchoring the surface free energy becomes infinite and the surface free energy terms in functional (1) should be replaced by suitable boundary conditions.

If the potential of the nematics-substrate interaction depends only on the angle between the director and the direction of anchoring of nematics molecules at the boundary, then the function $\vartheta = \vartheta(z)$ minimising the functional (1) must satisfy the Euler-Lagrange equations for it:

$$\begin{aligned} &\frac{\partial f}{\partial \vartheta} - \frac{d}{dz}\frac{\partial f}{\partial \vartheta'} = 0 && \text{for } 0 < z < d \\ &-\left(\frac{\partial f}{\partial \vartheta'}\right)_{|z=0} + \frac{df_1}{d\vartheta_1} = 0 && \text{for } z = 0 \\ &\left(\frac{\partial f}{\partial \vartheta'}\right)_{|z=d} + \frac{df_2}{d\vartheta_2} = 0 && \text{for } z = d \end{aligned} \tag{2}$$

The left-hand-side of each of these equations can be meant as a torque density. Particularly the two last can be interpreted as equations of the balance of the torques induced by the nematics-substrate interaction, e.g., $\tau_1(\vartheta(0)) = df_1/d\vartheta_1(\vartheta(0))$, with the torques from the bulk induced by external fields, e.g.,

$$T_b = \tau(\vartheta(0)) = \left(\frac{\partial f}{\partial \vartheta'}\right)(\vartheta(0),\vartheta'(0)) = \int_0^d \frac{\partial f}{\partial \vartheta}(\vartheta(z),\vartheta'(z))dz.$$

In such configuration, the density of the free energy of elastic deformation (in the form proposed by Frank, with three elastic constant) is given by

$$f_K = \frac{1}{2}\left(K_{11}\cos^2\vartheta + K_{33}\sin^2\vartheta\right)\vartheta'^2 \tag{3}$$

where K_{11}, K_{33} are the splay and bend Frank elastic constants [11,12].

The density of the free energy of the coupling between the director field and a static external magnetic field (a magnetic induction B of the direction determined by the angle ψ, as in Fig. 2) is equal to

$$f_M = -\frac{1}{2}\mu_0^{-1}\chi_a B^2 \sin^2(\vartheta + \psi), \tag{4}$$

by neglecting the constant term; $\chi_a = \chi_{||} - \chi_{\perp}$ is the anisotropy of the diamagnetic susceptibility and μ_0 is the vacuum magnetic permeability.

The density of the free energy of the coupling between the director field and an external electric field (as in Fig. 2), induced by a voltage U applied between the cell boundaries, can be written down in the form [1,2,11,12]

$$f_E = -\frac{1}{2}\frac{\varepsilon_0 \varepsilon_e^2 U^2}{d^2\left(\varepsilon_\perp \cos^2\vartheta + \varepsilon_{||}\sin^2\vartheta\right)},$$
$$\varepsilon_e = \left\{\frac{1}{d}\int_0^d \frac{1}{\varepsilon_\perp \cos^2\vartheta(z) + \varepsilon_{||}\sin^2\vartheta(z)}dz\right\}^{-1} \tag{5}$$

by neglecting the constant term; ε_e is the effective electric permittivity of the nematics layer (deformed by static external fields), $\varepsilon_\perp, \varepsilon_{||}$ are the electric permittivities of the nematics and ε_0 is the vacuum electric permittivity.

The tilt angle as a function of z should satisfy the Euler-Lagrange equations for the bulk-free-energy functional (1) [2,11,12], following from (2), (3), (4), (5):

$$\left(K_{11}\cos^2\vartheta + K_{33}\sin^2\vartheta\right)\vartheta'' + (K_{33}-K_{11})\sin\vartheta\cos\vartheta\cdot\vartheta'^2$$
$$+\frac{\varepsilon_0\varepsilon_a\varepsilon_e^2 U^2\sin\vartheta\cos\vartheta}{d^2\left(\varepsilon_\perp\cos^2\vartheta+\varepsilon_{||}\sin^2\vartheta\right)^2}+\frac{\chi_a B^2}{\mu_0}\sin(\vartheta+\psi)\cos(\vartheta+\psi)=0 \tag{6}$$
$$\varepsilon_e = \left\{\frac{1}{d}\int_0^d \frac{1}{\varepsilon_\perp \cos^2\vartheta(z) + \varepsilon_{||}\sin^2\vartheta(z)}dz\right\}^{-1}$$

where $\varepsilon_a = \varepsilon_{||} - \varepsilon_\perp$ is the anisotropy of electric permittivity. Since the nematics-substrate interaction is not taken into account in equations (6), function $\vartheta(z)$ should also satisfy a boundary condition [1,11,12], defining the dependence of the boundary values of ϑ on the elastic torque (per unit area), T_b, acting from the bulk to the boundaries:

$$T_b = \int_0^d \left[(K_{11}-K_{33})\sin\vartheta(z)\cos\vartheta(z)\vartheta'(z)^2\right]dz$$
$$+\int_0^d\left[\frac{\varepsilon_0\varepsilon_a\varepsilon_e^2U^2\sin\vartheta(z)\cos\vartheta(z)}{d^2\left[\varepsilon_\perp\cos^2\vartheta(z)+\varepsilon_{||}\sin^2\vartheta(z)\right]^2}\right.$$
$$\left.+\frac{\chi_a B^2}{\mu_0}\sin(\vartheta(z)+\psi)\cos(\vartheta(z)+\psi)\right]dz$$
$$\vartheta(0)=\vartheta(d)=\Theta(T_b). \tag{7}$$

The boundary function $\Theta(T_b)$ should be non-decreasing; previously it was approximated [1,2] by third-order polynomials, $\Theta(T_b) \cong \Theta_0 + \Theta_1 T_b + \Theta_2 T_b^2 + \Theta_3 T_b^3$, and in this work it is modelled by a first-order polynomial, $\Theta(T_b) \cong \Theta_0 + \Theta_1 T_b$, or a cubic spline, both non-decreasing.

Determination of Nematics Parameters by Solving Inverse Problem

Composite method [1,2] relies on solving an inverse problem for finding the magnitudes of material parameters (like the anisotropy of diamagnetic susceptibility, the splay and bend elastic constants and the characteristics of the nematics-substrate coupling), in both the cases of strong or weak anchoring, without any additional simplifications. Every electric or magnetic characteristics of a planar nematic cell as a birefringence system, i.e., the dependence of the phase shift $\varphi = \varphi(U; B, \psi)$ on nematics deformation,

$$\varphi = \frac{2\pi}{\lambda} d \left[\frac{1}{d} \int_0^d \frac{n_e \cdot n_o}{\sqrt{n_e^2 \cdot \sin^2 \vartheta(z) + n_o^2 \cdot \cos^2 \vartheta(z)}} dz - n_o \right], \qquad (8)$$

contains the information about material constants $K_{11}, K_{33}, \chi_a, \Theta$.

Let $p = (K_{11}, K_{33}, \chi_a, \Theta_0, \Theta_1, \Theta_2, \Theta_3)$ denote the set of unknown material parameters (in case of first-order polynomial, modelling the nematics-substrate interaction, only two coefficients Θ_0, Θ_1 are sought, in case of non-decreasing cubic spline the number of coefficients is greater than four). The polynomial or spline coefficients Θ are here model parameters and can be considered as material constants characterising a nematics-substrate system (and not a nematics itself). For any sequence of n measurements $\left(\varphi_e(U^i; B^i, \psi^i)\right)_{i=1}^n$ one can calculate a corresponding sequence of values of light phase shift $\left(\varphi_c(U^i; B^i, \psi^i; p)\right)_{i=1}^n$ using formulae (6), (7), (8). By minimising the similarity functional [1,2]:

$$S(p) = \left\{ \frac{1}{n} \sum_{i=1}^n \left[\frac{\varphi_e(U^i; B^i, \psi^i) - \varphi_c(U^i; B^i, \psi^i; p)}{\varphi_e(U^i; B^i, \psi^i))} \right]^2 \right\}^{1/2} \qquad (9)$$

one finds the unknown magnitudes of material parameters p. Using a wedge cell one can exploit few characteristics simultaneously, e.g., corresponding to different fringes, what makes results of computations more reliable especially when the nematics-substrate coupling is modelled by non-decreasing spline. Usually an approximate solution of this inverse problem is found with using the spline model of the nematics-substrate interaction (corresponding to the polar surface anchoring energy) and when it follows from the results that a third-order or first-order polynomial would provide equally good solution, the computations are repeated with using such more restricted polynomial model.

Determination of Nematics Parameters from Freedericksz Thresholds Magnitudes of Combined Electric and Magnetic Fields

Method of investigating the thresholds for Fréedericksz' transition [3,4,5] relies on comparing the threshold field magnitudes of a voltage (parameterised by a magnetic field) or of a magnetic field (parameterised by a voltage), corresponding to the same equivalent flat-parallel cell, for finding the anisotropy of diamagnetic susceptibility and the splay elastic constant, only in the case of strong nematics-substrate coupling and the anchoring direction equal to zero. The stationary states of a cell with a nematics of positive or negative anisotropy of diamagnetic susceptibility, χ_a, and positive anisotropy of electric permittivity ($\varepsilon_a > 0$), corresponding to weak external fields and small deformations, can be described by a linearised version of the Euler-Lagrange equations (2), (6). For magnetic field acting perpendicularly ($\psi = 0$) or parallel ($\psi = \frac{1}{2}\pi$) to the layer and $\vartheta(0) = \vartheta(d) = \vartheta_0 = 0$, one can approximate (assuming $\vartheta << 1$) $\sin\vartheta \approx \vartheta$, $\cos\vartheta \approx 1$, $\varepsilon_e \approx \varepsilon_\perp$ and finally

$$\vartheta''(z) + \omega^2\vartheta(z) = 0 \quad \text{for } 0 < \mathrm{z} < \mathrm{d}, \tag{10}$$

$$\vartheta(0) = 0, \vartheta(d) = 0,$$

where $\omega^2 \equiv \left[\varepsilon_0\varepsilon_a d^{-2}U^2 + \cos(2\psi)\mu_0^{-1}\chi_a B^2\right]K_{11}^{-1}$ and one assumes $\omega^2 > 0$.

This boundary-value problem has a non-zero solution $\vartheta(z) = C\sin(\omega z)$ only if the condition $\sin(\omega d) = 0$ is satisfied (C is an arbitrary constant). The last condition leads to the equation involving the pair of the threshold field magnitudes (i.e., of voltage and magnetic tension):

$$\pi^{-2}\varepsilon_0\varepsilon_a K_{11}^{-1}U_{th}^2 + \pi^{-2}\cos(2\psi)\mu_0^{-1}\chi_a K_{11}^{-1}(B_{th}d)^2 = 1. \tag{11}$$

The basic stationary state of the cell, enforced only by the boundary conditions is stable until the left-hand side of this equation, calculated for external fields applied to the cell, is less than 1.

Equation (11) defines the connexion between the threshold electric and magnetic tensions, U_{th} and $B_{th}d$, in the form of equation of an ellipse (when $\psi = 0$ for $\chi_a > 0$) or a hyperbole (when $\psi = 1/2\pi$ for $\chi_a > 0$). It can be written down in the following form:

$$\chi_a = \left(\pi^2 K_{11} - \varepsilon_0 \varepsilon_a U_{th}^2\right) \mu_0 \cos(2\psi) (B_{th} d)^{-2}, \qquad (12)$$

enabling the calculation of the magnitude of the anisotropy of diamagnetic susceptibility, given the anisotropy of electric permittivity ε_a, the splay elastic constant K_{11} and the threshold electric and magnetic tensions U_{th} and $B_{th}d$ measured. Taking into account several different measurements of U_{th} and corresponding $B_{th}d$ one can find the value χ_a more accurately by computing the arithmetic mean of all results; using a wedge cell one can exploit few different fringes (i.e., equivalent flat-parallel cells) simultaneously. On the other hand, exploiting the uniqueness of the definition of conical curve by its canonical equation, one can determine two of the three parameters χ_a, K_{11} or ε_a after the results of at least two measurements of different U_{th} and $B_{th}d$, for example χ_a, K_{11} (ε_a can be more easily determined from separate measurements). Different optimisation criteria, based on Eq. (11) or (12), can be applied for this purpose.

Determination of Nematics Parameters from Set of Freedericksz Threshold Magnitudes of Magnetic Field

Method of investigating the thresholds for magnetic Fréedericksz' transition ([7], analogous to presented in [6] for the electric case) relies on exploiting the threshold field magnitudes of a magnetic field, corresponding to different equivalent flat-parallel cells, for finding the anisotropy of diamagnetic susceptibility, the splay elastic constant and the polar anchoring energy coefficient, only in the case of weak coupling and the anchoring direction equal to zero. If the surface free energy density on both nematics layer surfaces is in accordance with the Rapini-Papoular formula (cf. e.g., [11,12]),

$$f_s(\vartheta_s) = \tfrac{1}{2} W \sin^2(\vartheta_s - \vartheta_0), \quad \vartheta_s \equiv \vartheta(0) \text{ or } \vartheta_s \equiv \vartheta(d), \qquad (13)$$

then the Euler-Lagrange Eq. (2), (6) takes the form of a system of equations:

$$\begin{aligned} &\left[K_{11} \cos^2 \vartheta(z) + K_{33} \sin^2 \vartheta(z)\right] \vartheta''(z) \\ &\quad + (K_{33} - K_{11}) \sin \vartheta(z) \cos \vartheta(z) \cdot (\vartheta'(z))^2 \\ &\quad + \chi_a \mu_0^{-1} B^2 \sin(\vartheta(z) + \psi) \cos(\vartheta(z) + \psi) = 0 \qquad \text{for } 0 < z < d, \end{aligned} \qquad (14)$$

$$
\begin{aligned}
&-\left[K_{11}\cos^2\vartheta(0)+K_{33}\sin^2\vartheta(0)\right]\vartheta'(0)\\
&\quad+W\sin(\vartheta(0)-\vartheta_0)\cos(\vartheta(0)-\vartheta_0)=0,\\
&\left[K_{11}\cos^2\vartheta(d)+K_{33}\sin^2\vartheta(d)\right]\vartheta'(d)\\
&\quad+W\sin(\vartheta(d)-\vartheta_0)\cos(\vartheta(d)-\vartheta_0)=0.
\end{aligned}
$$

The stationary states of a cell with a nematics of positive anisotropy of diamagnetic susceptibility ($\chi_a > 0$), corresponding to weak magnetic fields acting perpendicularly to the layer ($\psi = 0$) and small deformations, can be described by a linearised version of the Euler-Lagrange equations; if $\vartheta_0 = 0$ and $\vartheta << 1$ then $\sin\vartheta \approx \vartheta$, $\cos\vartheta \approx 1$ and

$$
K_{11}\vartheta''(z)+\mu_0^{-1}\chi_a B^2\vartheta(z)=0 \quad \text{for} \quad 0<z<d, \tag{15}
$$

$$
K_{11}\vartheta'(0)-W\vartheta(0)=0,
$$

$$
K_{11}\vartheta'(d)-W\vartheta(d)=0.
$$

This system has a solution of the form $\vartheta(z) = C_1\cos\omega z + C_2\sin\omega z$, being a solution of the first equation with $\omega^2 \equiv \mu_0^{-1}\chi_a B^2 K_{11}^{-1}$ and constants C_1 and C_2 satisfying the two others equations. This implies the condition for the stability of the basic stationary state [7]: it is stable until magnetic field is greater than the Fréedericksz threshold for weak anchoring, B_w, being the smallest root of the characteristic equation:

$$
\frac{\sqrt{\mu_0^{-1}\chi_a K_{11}}}{W\cdot d}\cdot B_w\cdot d=\cot\left(\frac{1}{2}\sqrt{\frac{\chi_a}{\mu_0 K_{11}}}\cdot B_w\cdot d\right). \tag{16}
$$

The last equation can be written down in the following form, in which both sides depend linearly on cell thickness d:

$$
\begin{aligned}
W\cdot d &= \sqrt{\mu_0^{-1}\chi_a K_{11}}\cdot B_w\cdot d\cdot\tan\left(\frac{1}{2}\sqrt{\frac{\chi_a}{\mu_0 K_{11}}}\cdot B_w\cdot d\right)\\
&\equiv f_w(\chi_a, K_{11}; B_w d).
\end{aligned} \tag{17}
$$

The polar anchoring energy coefficient W can be calculated from this equation after the dependence of magnetic tension $B_w \cdot d$ on cell thickness d, for the values of other parameters, K_{11} and χ_a, given. Moreover, it is observed that the curve $f_w(d)$ is not linear for the given set of B_w and d measured unless both the parameters K_{11} and χ_a have the proper values; this can be exploited to determine both W and one of the parameters K_{11} or χ_a simultaneously (given the other).

Formula (13) implies $T_b = df_s/d\vartheta_s(\vartheta_s) = W\sin(\vartheta_s - \vartheta_0)\cos(\vartheta_s - \vartheta_0) \approx W(\vartheta_s - \vartheta_0)$ and $\vartheta_s \approx \vartheta_0 + W^{-1}T_b$ for small ϑ_s and ϑ_0, what gives $\vartheta_0 = \Theta_0, W = \Theta_1^{-1}$ when $\vartheta_s(T_b) = \Theta_0 + \Theta_1 T_b$.

Determination of Nematics Parameters by Comparing Deformations Induced by Electric and Magnetic Fields

Method of investigating optically equivalent nematics deformations [8] relies on comparing the energy of electric-induced deformation with the energy of magnetic-induced one, corresponding to the same optical response of the same equivalent flat-parallel cell, for finding the anisotropy of diamagnetic susceptibility, in both the cases of strong or weak coupling. The contributions from electric and magnetic fields to the density of the bulk free energy functional can in general be described as follows: $f_E = -1/2\varepsilon_0\varepsilon_a\vec{E}\cdot\vec{n}$ and $f_M = -1/2\mu_0^{-1}\chi_a\vec{B}\cdot\vec{n}$. Analysing the form of the Euler-Lagrange Eq. (6) and the final forms of f_M (4) and f_E (5) in one-dimensional approximation, one can conclude the approximate equality [8,9,10]

$$\chi_a\mu_0^{-1}B^2 = \varepsilon_a\varepsilon_0 U^2 d^{-2}, \tag{18}$$

which can be applied for determining the anisotropy of diamagnetic susceptibility, χ_a, given the values of the others quantities involved. Due to the forms of formulae (4), (5), (6) it is rather difficult to estimate the accuracy of this method for determining χ_a, interesting for the simplicity of formula (18).

MEASUREMENT SYSTEM

The scheme of measurement system is presented in Figure 3. It makes possible the measurements of a nematic cell in two different positions, with a magnetic field (i.e., magnetic induction B) parallel ($\psi = 1/2\pi$) or perpendicular ($\psi = 0$) to the cell boundaries. An electric field (and electric induction) is always perpendicular to the boundaries, as induced by a voltage applied between them. A low-frequency (1.5 kHz) sinusoidal voltage is used instead of a constant one.

RESULTS OF MEASUREMENTS AND COMPUTATIONS

Two wedge cells were filled with 4′-pentyl-4-cyanobipfenyl (5CB). Two polyimide, poly(amic acid) PM9 and MP2 [13], were used as aligning substances. The orienting surfaces were prepared by rubbing in the direction parallel to the wedge edge.

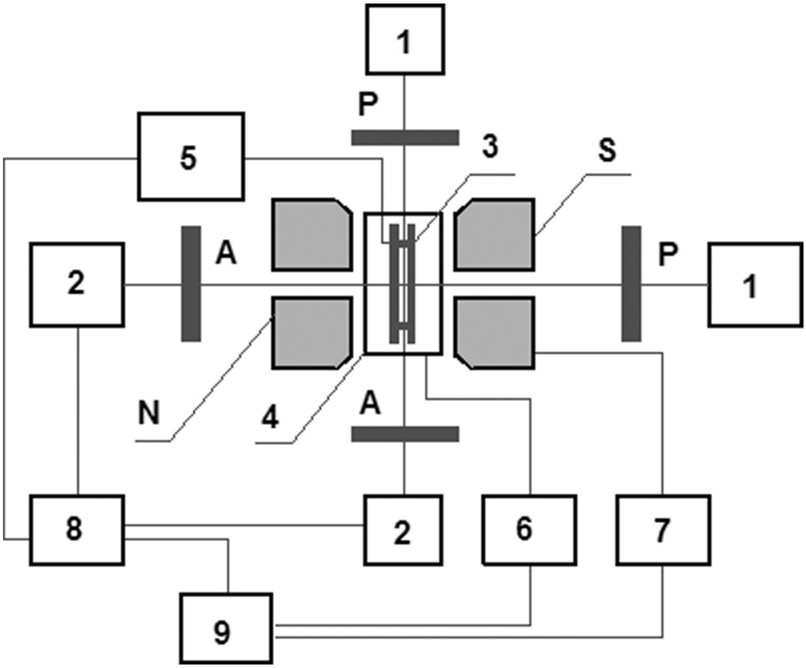

FIGURE 3 Block diagram of the measurement system for studying nematics deformations in magnetic and electric fields; 1 – the NG HN 25/40 He–Ne laser, 2 – the projection objective, 3 – the liquid crystal cell, 4 – the thermostatic measuring chamber, 5 – the HP33120A function generator or the HP4284A precision RLC meter, 6 – the Heto CB7 thermo-stabiliser, 7 – the Radiopan PZP8005 electro-magnet power supply with the current control unit, 8 – the PZO MB30 microscope with the photodetector and the Meratronik V543 digital voltmeter, 9 – the computer system with the IEEE 488 bus for recording results; A – the analyser, P – the polariser (two positions exploited in measurements are shown); N, S – the electromagnet poles.

The intensity of light normally incident at the cell boundaries, transmitted through the birefringence system (Fig. 3), as a function of a magnetic field B, perpendicular to the cell boundaries ($\psi = 0$), was recorded for six interference fringes (8–13, corresponding to the cell thickness $27.6\,\mu m \div 44.9\,\mu m$) in the 5CB-PM9 cell (at the temperature 22.3°C) and for six fringes (6–11, corresponding to the cell thickness $20.9\,\mu m \div 38.2\,\mu m$) in the 5CB-MP2 cell (at the temperature 22.7°C), moreover it was recorded as a function of a voltage parameterised by a constant magnetic field of different magnitudes for six interference fringes (two times each of 9, 11 and 13) in the 5CB-PM9

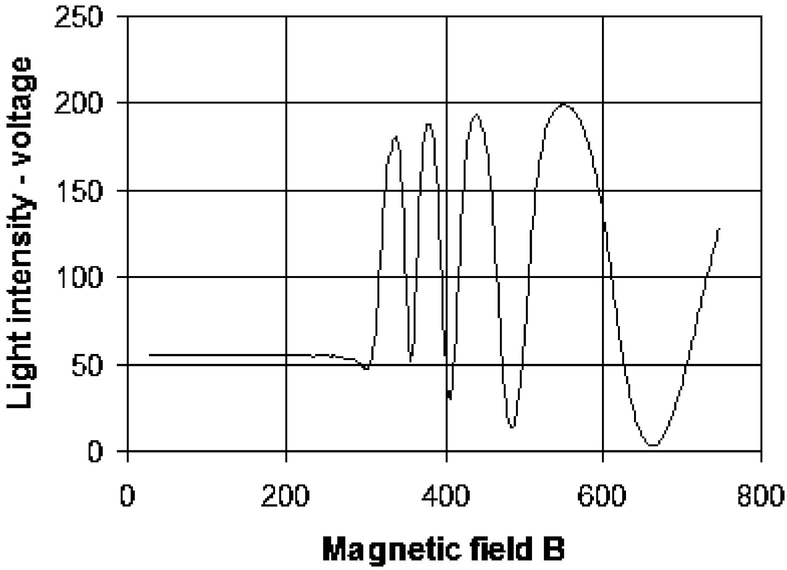

FIGURE 4 Intensity of normally incident light (expressed as equivalent voltage in mV), transmitted through the 5CB-MP2 cell in the place of the appearance of sixth interference fringe, corresponding to the cell thickness 20.9 μm, as a function of a magnetic field B (in mT), at the temperature 22.7°C.

cell (at the temperature 22.3°C) and as a function of a voltage for six fringes (8–13) in the 5CB-PM9 cell (at the temperature 22.3°C) and six fringes (6–11) in the 5CB-MP2 cell (at the temperature 22.7°C). The temperature was stabilised with accuracy within 0.2°C. The driving external force (i.e., a magnetic field or a voltage) was changed during measurements so slowly that all deformation states could be considered as static caused by static external fields. An example characteristics is showed in Figure 4; the subsequent extreme points of such curve corresponds to the light phase shift φ (8) equal to integer multiplicities of π rad, as it is presented in Figure 5 (the first point corresponding to the threshold for Fréedericksz' transition is found by extrapolating a line after the four following points). The values of the phase shift as a function of an external field applied (i.e., magnetic in this case) are determined by finding the positions (abscissas) of the extreme points. The electric permittivities and the ordinary and extraordinary refraction indices of the 5CB nematics were measured in separate experiments. The sets of pairs (B, φ) or (U, φ) (or triples (U, B, φ)) were input data for extracting the sought values of material parameters by the methods A, B, C, D, described above.

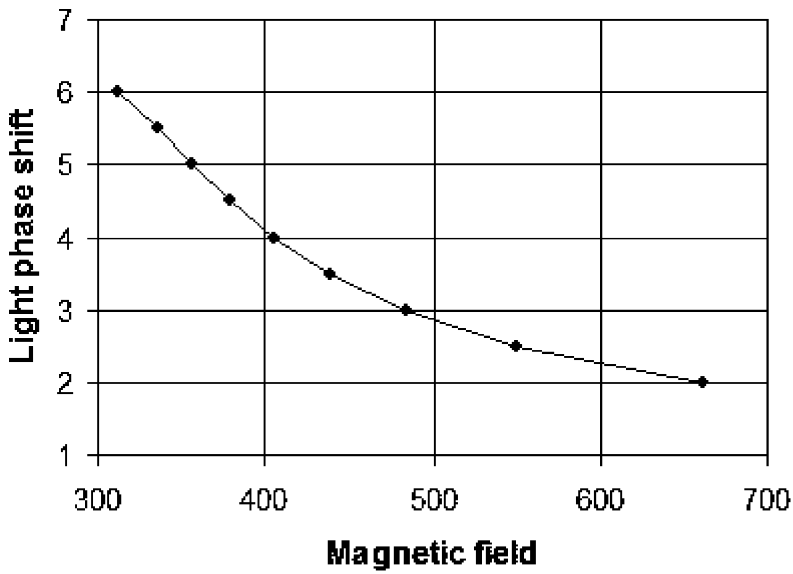

FIGURE 5 Phase shift (in 2π rad units) corresponding to subsequent extreme points of the curve in Figure 4 as a function of an applied magnetic field B (in mT); the Fréedericksz threshold field magnitude for weak anchoring is determined as corresponding to that of the biggest shift (i.e., zero-order minimum) and found by linear extrapolation from the four subsequent extreme points (this part of the curve is approximately linear).

The precise estimation of errors in resulting numerical values is difficult due to complicated procedures of measurements and computations. Comparing results of intermediate measurements, computations and simulations one can expect the relative errors not exceeding the following magnitudes: 0.001 in n_0, n_e; 0.01 in $d, t, \varepsilon_\perp, \varepsilon_{||}$; 0.03 in K_{11}; 0.05 in K_{33}, χ_a and 0.1 in ϑ_0, W. In the numerical values presented above and below one excessive digit is mostly preserved to avoid additional rounding errors and to show better the differences.

Method A

The computations were done to achieve approximately the best-possible fit of characteristics, calculated with the same values of the nematics parameters and two functions characterising the nematics-substrate coupling (for 5CB-PM9 and 5CB-MP2 systems), to the experimental ones (i.e., measured for all analysed interference fringes). The best results were obtained by modelling the dependence of the boundary tilt angle on

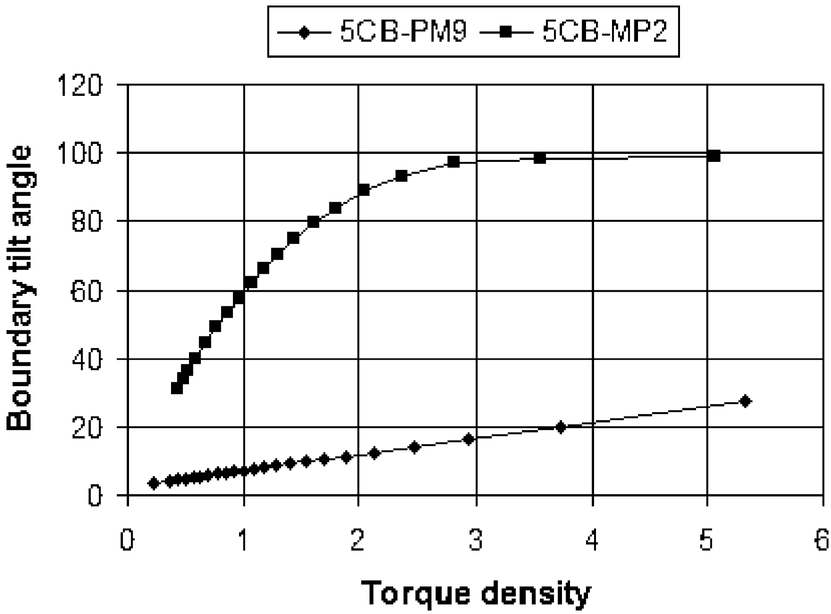

FIGURE 6 Director boundary tilt angle (in mrad) as a function of torque density $\vartheta(0) = \vartheta(d) = \Theta(T_b)$ (in $\mu J\, m^{-2}$), describing approximately the coupling between the nematics (5CB) and the substrate material (polyimide MP9 or polyimide PM2) at the boundaries of each equivalent planar cell.

the torque density as linear for 5CB-PM9 and as a non-decreasing cubic spline for 5CB-MP2 (Fig. 6). The material constants of 5CB at the temperature 22.3°C were following: $\varepsilon_{||} = 19.10$, $\varepsilon_{\perp} = 6.48$, $n_o = 1.5381$ and $n_e = 1.7215$, determined from previous measurements, and $K_{11} = 6.46\,pN$, $K_{33} = 8.85\,pN$ and $\chi_a = 1.67 \cdot 10^{-6}$, obtained as the solution of the inverse problem for the 5CB-PM9 cell (with $S(p) \approx (0.007 \div 0.022)$); at the temperature 22.7°C they were following: $\varepsilon_{||} = 19.03$, $\varepsilon_{\perp} = 6.50$, $n_o = 1.5383$ and $n_e = 1.7204$, determined from previous measurements, and $K_{11} = 6.47\,pN$, $K_{33} = 8.80\,pN$ and $\chi_a = 1.56 \cdot 10^{-6}$, obtained as the solution of the inverse problem for the 5CB-MP2 cell (with $S(p) \approx (0.007 \div 0.030)$. The anchoring angles $\vartheta_0 = \Theta_0$ and the polar anchoring energy coefficients $W \approx \Theta_1^{-1}$ were estimated by modelling (for 5CB-PM9) or approximating (for 5CB-MP2) $\Theta(T_b) \approx \Theta_0 + \Theta_1 T_b$ and extrapolating this function linearly to zero. They were following: 2.6 mrad and 215 $\mu J\, m^{-2}$ for 5CB-PM9 (strong anchoring); 8.2 mrad and 18.7 $\mu\, Jm^{-2}$ for PCB-MP2 (medium-weak anchoring). The boundary functions, describing the dependence of the tilt angle (i.e., director) at the boundaries on the elastic torque density, are shown in Figure 6. These results serve as the reference values for the magnitudes of material parameters determined by the other methods.

Method B

The method described above was applied for determining the anisotropy of diamagnetic susceptibility χ_a, or χ_a and the splay elastic constant K_{11} together, after the threshold voltages for the electric Fréedericksz transition parameterised by a magnetic field perpendicular to the cell boundaries, corresponding to 9th, 11th and 13th fringe in the 5CB-PM9 cell (two measurement for each fringe, at the temperature 22.3°C). In the first case the magnitude χ_a was found as the arithmetic mean of the set of its approximations calculated after formula (12), given K_{11}. In the second case additionally the K_{11} was determined by finding its magnitude corresponding to the minimal experimental standard deviation for the set of the results of calculating $\chi_a = \chi_a(U_{th}, B_{th}d)$ with respect to and in relation to the arithmetic mean of them. There were obtained $K_{11} = 6.46\,\mathrm{pN}$ and $\chi_a = 1.73 \cdot 10^{-6}$ (by calculating only χ_a; the results are presented in Table 1) or $K_{11} = 6.44\,\mathrm{pN}$ and $\chi_a = 1.72 \cdot 10^{-6}$ (by calculating both K_{11} and χ_a).

Method C

The magnitudes of the polar anchoring energy coefficient W and the anisotropy of diamagnetic susceptibility χ_a were found as a solution of equation (16) by non-linear least-square fitting of the value of χ_a, with using the values of magnetic tension experimentally determined as a function of the cell thickness for the 5CB-MP2 cell (i.e., for six fringes, 6–11, corresponding to the cell thickness $20.9\,\mu\mathrm{m} \div 38.2\,\mu\mathrm{m}$, at the temperature 22.7°C), to obtain the best linear approximation

TABLE 1 Results of Measurements of the Optical Response of the 5CB-PM9 Cell (at the Temperature 22.3°C) and the Computed Values of the Anisotropy of Diamagnetic Susceptibility; on Average $\chi_a = 1.73 \cdot 10^{-6}$

Fringe index j	9	9	11	11	13	13
Cell thickness d [μm]	31.1	31.1	38.0	38.0	44.9	44.9
Magnetic field B [T]	0.092	0.142	0.092	0.142	0.092	0.129
Threshold voltage U [V]	0.680	0.555	0.655	0.455	0.621	0.401
χ_a	$1.86 \cdot 10^{-6}$	$1.90 \cdot 10^{-6}$	$1.63 \cdot 10^{-6}$	$1.76 \cdot 10^{-6}$	$1.53 \cdot 10^{-6}$	$1.71 \cdot 10^{-6}$

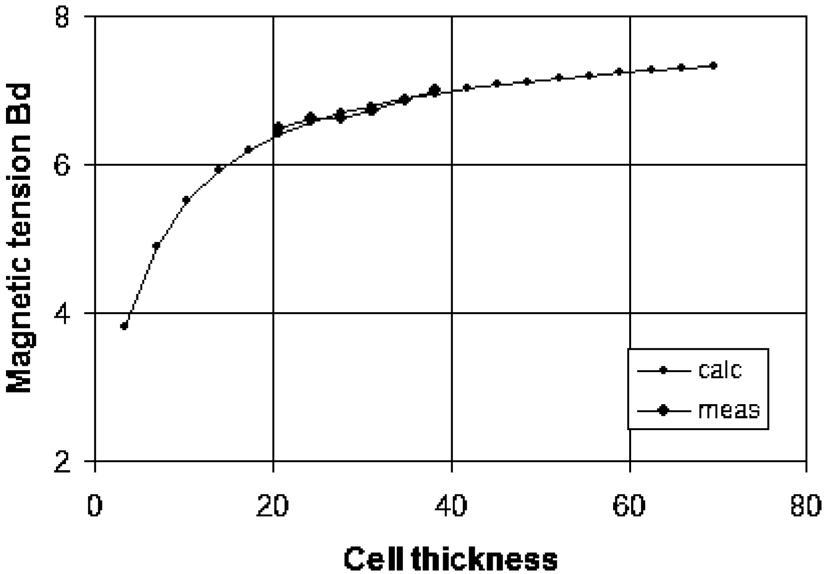

FIGURE 7 Magnetic tension (in mTm) as a function of the cell thickness (in μm), measured and calculated by using values of W and χ_a from fitting (the same as in Figure. 8).

of function f_w, and calculating W as the slope coefficient of this direct line (Fig. 8), given K_{11}. Good agreement of simulated and measured values of magnetic tension was achieved (Fig. 7). There were obtained $\chi_a = 1.56 \cdot 10^{-6}$ and $W = 3.27\,\mu\mathrm{J\,m^{-2}}$ by taking $K_{11} = 7.67\,\mathrm{pN}$ or $\chi_a = 1.32 \cdot 10^{-6}$ and $W = 2.76\,\mu\mathrm{J\,m^{-2}}$ by taking $K_{11} = 6.47\,\mathrm{pN}$, or $W = 3.01\,\mu\mathrm{J\,m^{-2}}$ and $\chi_a = 1.44 \cdot 10^{-6}$ by taking $K_{11} = 7.07\,\mathrm{pN}$ (as referred to in Fig. 7), all results with the same precision of fitting the function f_w by a linear function. It illustrates possible accuracy of the method. The disagreement between the magnitudes of the polar anchoring energy coefficient, obtained by this method and by more complicated and more accurate method A can be attributed to the lack of values of the light phase shift corresponding to the magnetic field magnitudes close to the threshold one, and moreover to the influence of non-zero anchoring angle (about 8.2 mrad).

Method D

The pairs of the magnitudes of a voltage and a magnetic field, measured for interference fringes from 6th to 11th in the 5CB-MP2 cell (at the temperature 22.7°C) and for interference fringes from

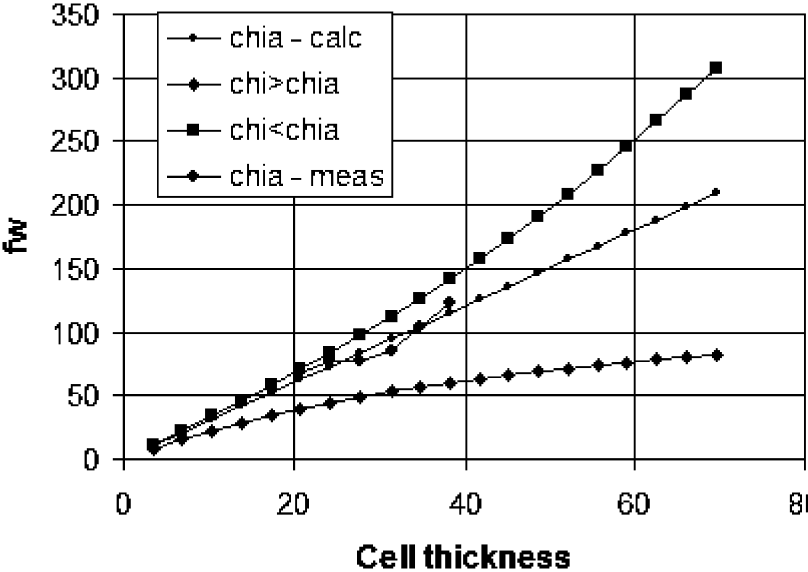

FIGURE 8 Right-hand-side of formula (17) calculated (in pN) for the threshold magnetic fields measured for six equivalent flat-parallel cells (i.e., for the interference fringes from 6th to 11th, corresponding to the cell thickness $20.9 \div 38.2\,\mu\mathrm{m}$), and simulated, by using the magnitudes $W = 3.01\,\mu\mathrm{Jm}^{-2}$ and $\chi_a = 1.44 \cdot 10^{-6}$ from fitting with assumed $K_{11} = 7.07\,\mathrm{pN}$. The two additional curves show the values of this function corresponding to the same values of all parameters except of χ_a taken greater or smaller than the former one obtained from fitting procedure.

8th to 13th in the 5CB-PM9 cell (at the temperature 22.3°C) as corresponding to the same phase shift of transmitted light (from its maximal value down to 4π rad and 6π rad) were used for determining

TABLE 2 Magnitudes of a Magnetic Induction and a Voltage in the 5CB-MP2 Cell and the Magnitudes of the Anisotropy of Diamagnetic Susceptibility χ_a Determined after them, Corresponding to the Maximums of the Optical Response Curve from 8th Fringe; the Mean Value Determined after all Fringes Involved $\chi_a = 1.78 \cdot 10^{-6}$

Light phase shift φ [2π rad]	7	6	5	4	3	2
Magnetic field B [T]	0.261	0.285	0.317	0.364	0.445	0.633
Voltage U [V]	0.815	0.924	1.043	1.191	1.403	1.799
χ_a	$1.76 \cdot 10^{-6}$	$1.90 \cdot 10^{-6}$	$1.96 \cdot 10^{-6}$	$1.93 \cdot 10^{-6}$	$1.90 \cdot 10^{-6}$	$1.46 \cdot 10^{-6}$

TABLE 3 Magnitudes of the Anisotropy of Diamagnetic Susceptibility χ_a Determined as the Averages after the Magnitudes for a Magnetic Induction and a Voltage in the 5CB-PM9 Cell Corresponding to the Extremes of the Optical Response Curves from 8th to 13th fringes; the Mean Value Determined after all Fringes Involved $\chi_a = 1.78 \cdot 10^{-6}$

Fringe index j	8	9	10	11	12	13
Cell thickness d [μm]	27.6	31.1	34.5	38.0	41.4	44.9
χ_a	$1.69 \cdot 10^{-6}$	$1.70 \cdot 10^{-6}$	$1.72 \cdot 10^{-6}$	$1.73 \cdot 10^{-6}$	$1.75 \cdot 10^{-6}$	$1.75 \cdot 10^{-6}$

TABLE 4 Magnitudes of Anisotropy of Diamagnetic Susceptibility Determined by the Four Methods Applied

Method	5CB-PM9 22.3°C	Relative deviation	5CB-MP2 22.7°C	Relative deviation
A	$1.67 \cdot 10^{-6}$	0	$1.56 \cdot 10^{-6}$	0
B	$1.73 \cdot 10^{-6}$	0.04		
C			$1.32 \cdot 10^{-6}$	−0.15
D	$1.73 \cdot 10^{-6}$	0.04	$1.78 \cdot 10^{-6}$	0.14

the magnitude of the anisotropy of diamagnetic susceptibility χ_a, in accordance with formula (18). The arithmetic mean from all results implies the value $\chi_a = 1.78 \cdot 10^{-6}$ (at the temperature 22.7°C) or $\chi_a = 1.73 \cdot 10^{-6}$ (at the temperature 22.3°C). Examples of the results of measurements and computations are showed in Table 2 for the 5CB-MP2 cell (only the magnitudes of χ_a determined after the maximums of the optical response curve from 8th fringe) and in Table 3 for the 5CB-PM9 (the magnitudes of χ_a determined as the averages after the extremes of the optical response curves from 8th to 13th fringes).

CONCLUSION

The magnitudes of the anisotropy of diamagnetic susceptibility χ_a, obtained by all methods presented above are collected in Table 4; those obtained by method A are treated as the reference values. For methods B and C the presented magnitudes of χ_a correspond to the magnitudes of K_{11} the same as determined by method A, although the magnitude of K_{11} at the temperature 22.7°C should be rather a little smaller than that at the temperature 22.3°C.

Good agreement between the values of nematics material parameters determined by each of these methods was achieved (at the level of about 10%). The differences may be attributed to inaccuracy of determining the positions of extreme points of transmitted light intensity (up to about 3 mT or 3 mV), to inaccuracy of determining the temperature of the measurement stage (within 0.2°C) and to the simplified assumption made in deriving the basic formulae of methods B, C and D.

REFERENCES

[1] Kędzierski, J., Kojdecki, M. A., Raszewski, Z., Perkowski, P., Rutkowska, J., Piecek, W., Lipińska, L., & Miszczyk, E. (2000). *Mol. Cryst. Liq. Cryst.*, *352*, 77–84.
[2] Kędzierski, J., Kojdecki, M. A., Raszewski, Z., Lipińska, L., Rutkowska, J., Miszczyk, E., & Borycki, J. (2004). *Mol. Cryst. Liq. Cryst.*, *409*, 301–314.
[3] Schadt, H., Baur, G., & Meier, G. (1979). *J. Chem. Phys.*, *71*, 3174–3181.
[4] Schadt, H., Baur, G., & Meier, G. (1979). *J. Chem. Phys.*, *70*, 2770–2774.
[5] Kędzierski, J., Raszewski, Z., Kojdecki, M. A., Zieliński, J., Miszczyk, E., Perkowski, P., Piecek, W., & Lipińska, L. (2004). *Proceedings of SPIE*, *5565*, 246–250.
[6] Gu, D. F., Uran, S., & Rosenblatt, C. H. (1995). *Liq. Cryst.*, *19*, 427–431.
[7] Kędzierski, J., Raszewski, Z., Kojdecki, M. A., Zieliński, J., Miszczyk, E., & Lipińska, L. (2004). *Opto-Electronics Review*, *12*(3), 299–303.
[8] Tsvetkov, V. N., Ryumtsev, E. I., Kolomiyets, I. P., & Kovshik, A. P. (1973). *An USSR Doklady*, *211*, 821–824.
[9] Haase, W. (2001). In: *Liquid Crystals: Nematics*, Dunmur, D. A., Fukuda, A., & Luckhurst, G. R. (Eds.), INSPEC, IEE: London, Chapter 6.3, 288–296.
[10] Zocher, H. (1933). *Trans. Faraday Soc.*, *29*, 945–957.
[11] de Gennes, P. G. & Prost, J. (1993). *The Physics of Liquid Crystals*, Oxford University Press: Oxford.
[12] Blinov, L. M. & Chigrinov, V. G. (1994). *Electrooptic Effects in Liquid Crystal Materials*, Springer Verlag: New York.
[13] Borycki, J., Wilczek, M., Kędzierski, J., & Kojdecki, M. A. (2004). *Proceedings of SPIE*, *5565*, 354–358.